

Dynamic Performance of a Magnetic Levitation Haptic Device

P. Berkelman and R.L. Hollis*

The Robotics Institute
Carnegie Mellon University
Pittsburgh, PA 15213

ABSTRACT

A new haptic interface device has been developed which uses Lorentz force magnetic levitation for actuation. With this device, the user grasps a floating rigid body to interact with the system.

The levitated moving part grasped by the user contains curved oval wound coils and LEDs embedded in a hemispherical shell with a handle fixed at its center. The stationary base contains magnet assemblies facing the flotor coils and optical position sensors facing the flotor LEDs. The device is mounted in the top cover of a desk-side cabinet enclosure containing all the amplifiers, control hardware, microprocessing, and power supplies needed for operation. A network connection provides communication with a workstation to allow interaction with simulated 3D environments in real time.

Ideally, the haptic interface device should reproduce the dynamics of the modelled or remote environment with such high fidelity that the user cannot distinguish interaction with the device from interaction with a real object in a real environment. In practice, this ideal can only be approached with a fidelity that depends on its dynamic properties such as position and force bandwidths, maximum forces and accelerations, position resolution, and realizable impedance range.

The motion range of the moving part is approximately 25 mm and 15-20 degrees in all directions. A current of 0.75 A is required in three of the six coils to generate the vertical force to lift the 850 g levitated mass, dissipating only 13.5 W. Peak forces of over 50 N and torques of over 6 Nm are achievable with the present amplifiers without overheating the actuator coils. Other measured performance results include stiffness ranges from 0.005 N/mm to 25.0 N/mm and a position control bandwidth of approximately 75 Hz.

Keywords: haptic, magnetic levitation

1. INTRODUCTION

The haptic sense is a combination of tactile sensing which is local sensation from nerve receptors in the skin, and kinesthetic sensing, which is due to internal distributed sensation in the joints and muscles. Humans use dexterous motion of the hand together with the sense of touch and feel to gain information about the dynamics and surface characteristics of the environment when we grasp, squeeze, push, pick up, manipulate, or touch the surface of objects. The synthesis of haptic sensing with dexterous motion comprises *haptic exploration* or *haptic interaction*. Comprehensive surveys of psychophysical, perceptual, sensitivity and bandwidth issues in human haptic sensing are given by Shimoga and Cholewiak and Collins.^{1,2}

Potential applications of haptic interaction include CAD, biomolecular analysis, medical simulation, and entertainment. A haptic interface to a CAD system would enable a user to directly feel subtleties of the fit, surface finish, and inertia of modelled parts. Haptic interaction with a medical simulation would allow a surgeon in training to realistically feel and manipulate body tissues. With a haptic interface a user could move in and feel any arbitrary properties representable as a vector field, such as fluid flow, pressure, magnetic field, or any potential field gradient.

The new magnetic levitation haptic interface device was built for high-performance, tool-based haptic interaction with physical environment simulations. In tool-based haptic interaction, the user feels and interacts with the simulated environment through a rigid tool of a given shape rather than directly with the hand and fingers. Consequently, a tool-based haptic interaction device only needs to control the dynamics of the rigid-body tool grasped by the user,

* pjb@ri.cmu.edu, rhollis@ri.cmu.edu

rather than stimulate the user’s skin, joints, or muscles directly. Tool-based human tasks such as cutting, pushing, screwing, probing, and inserting can all be simulated with tool-based haptic interaction.

An ideal haptic interface would enable simulated virtual objects to be sensed and manipulated in exactly the same natural and intuitive manner as are real objects in the world. The high dexterity and sensitivity of the hand provides a rich and direct medium for interaction between the user and the simulated world. Psychophysical studies have shown that the haptic sensitivity of the human hand extends to the micron level with a bandwidth of at least several hundred Hertz.^{1,2} To realistically emulate the experience of handling real objects, the haptic interface system must reproduce object dynamics at the same high level of detail and responsiveness. To achieve this performance requires a device with stiff and lightweight moving parts, powerful and responsive actuators, high resolution sensors, and a fast, low latency control system.

The most important performance criteria for a haptic interaction device are its sensitivity, or position resolution, and its responsiveness, or control bandwidths. We propose that Lorentz levitation technology is especially well suited to high-performance tool-based haptic interaction because it provides motion and force feedback in 6 DOF with very high control bandwidths and sensitivity, non-contact actuation and position sensing, and only one moving part.³ The magnetic levitation haptic interaction system under development provides a comfortable range of motion for the fingertips for fine haptic tasks and is totally enclosed in a desktop-height cabinet.

2. PREVIOUS HAPTIC INTERACTION DEVICES

The development of haptic interface devices began from large, heavy serial manipulators used as force-reflecting hand controller masters and has progressed to increasingly fast, lightweight, and sensitive linkage, and tensioned cable devices as well as exoskeletons and tactile displays. The main reported performance parameters of several existing force/kinesthesia based devices are summarized in Table 1.

2.1. Cable and Linkage Devices

Tensioned cable systems for haptic interaction have been developed at JPL, Tokyo Institute of Technology, and the University of Texas at Austin.⁴⁻⁶ In these systems, a handle grasped by the user is supported from all directions by several actuated cables. The combined tension in the cables produces a net force and torque on the user’s hand. The workspace of the device can be made very large while the actuated inertia remains small.

A lightweight 3 DOF linkage called the PHANToM was developed at MIT and is commercially produced by SensAble Technologies, Inc.⁷ The user interacts with this device through a fingertip thimble or grasped stylus. An optional encoder gimbal adds 3 DOF of orientation sensing but no feedback torques. The Pantograph, developed at McGill University, is a small 2 DOF planar linkage with low inertias and reported to be capable of high bandwidths.⁸

A 6 DOF platform called the HapticMaster was developed by Iwata at the University of Tsukuba and is commercially produced by Nissho Electronics.⁹ The moving platform of this device is supported by three 3 DOF pantograph linkages, resulting in redundant actuation with 9 DOF. A compact pen-based 7 DOF linkage and tendon device is under development at McGill University which aims to provide dynamic response to 50-100 Hz, forces from 1 mN to 10 N, and variation in mechanical impedance over 3 orders of magnitude.¹⁰

2.2. Magnetic Levitation Devices

Earlier magnetic levitation devices have used Lorentz force magnetic levitation technology. The levitated part of these devices is referred to as the *flotor* while the stationary base containing the permanent magnet assemblies is the *stator*. This means of haptic interaction has previously been demonstrated with the IBM Magic Wrist and the UBC wrist,^{11,12} shown in Figures 1 and 2.

The first Lorentz force magnetic levitation device was the Magic Wrist developed at IBM T.J. Watson Research Center. This device was originally designed as a fine-motion robot wrist for coarse-fine manipulation and later adapted for use as a haptic interface for mechanism emulation, solid contacts, and texture and friction experiments.¹³ The magnet assemblies in this device are arranged in inner and outer rings and the flotor coils are embedded in the sides of a hexagonal box. Three position sensing photodiodes on the inside of the flotor and three narrow-beam LEDs on the stator are used for position sensing. Its force, motion, and bandwidth parameters are also given in Table 1.

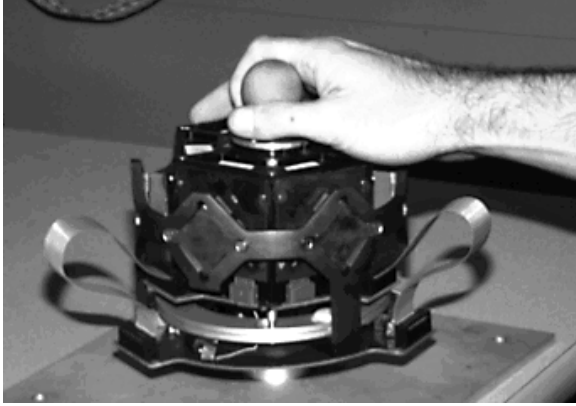


Figure 1. Magic Wrist

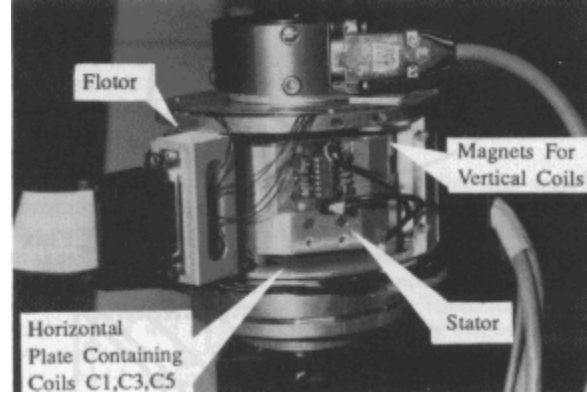


Figure 2. UBC Wrist

Device Type	DOF	Force Range	Motion Range	Bandwidth	Resolutions
Texas 9-string	6	43.4 N, 4.8 N-m	450 mm dia. sphere	<10 Hz pos.	NA
SPIDAR II	6-12	4 N/cable	300 mm dia. sphere	30 Hz force	0.5 mm
NWU Stewart Platform	4	45 N, 1.35 N-m	200x80 mm	<100 Hz	0.05°
U. Tsukuba Pen	6	5 N	440 mm dia. sphere	<10 Hz pos.	2 mm
PER-Force	6	53 N	100 mm, 90-180°	100 Hz	7.5 μm, 0.01°
PHANToM	3	8.5 N	130x180x250 mm	800 Hz force	0.03 mm
HapticMaster	6	69 N, 0.5 N-m	400 mm dia. sphere	50 Hz force	0.4 mm
Magic Wrist & UBC Wrist	6	20N	±4.5 mm, ±6°	15-50 Hz pos. 3000 Hz force	< 5μm
Proposed Device	6	60 N, 3 N-m	> 25 mm sphere, ±12°	> 100 Hz pos.	3 μm

Data taken from Burdea¹⁵ and others.

Table 1. Published Haptic Interface Device Parameters

Due to the hexagonal shape of the flotor, the ranges of motion in translation and rotation are not independent. At the maximum translation the rotation range decreases to zero, and similarly there is no translation range at the maximum rotation because the edges and corners of the hexagonal box flotor collide with the magnet assemblies. These limitations of the Magic Wrist are not a problem when the wrist is carried by a 6 DOF robot arm, but as a haptic interface device it is difficult for the user to haptically recognize shape features scaled down to a motion range of under 10 mm.

The UBC Wrist is another 6 DOF Lorentz force magnetic levitation device that has been used as a teleoperation master, as a fine motion wrist, and for haptic interaction.¹⁴ The UBC wrist is smaller and has a more compact arrangement of actuators but it has a similar cylindrical shape. Its mass is 0.65 kg and position and force control bandwidths and ranges of force and motion are similar to the Magic Wrist. Both the IBM Magic Wrist and the UBC Wrist were designed as compact fine motion robot wrists for high position accuracy and sensitivity, so their limited motion range and non-ergonomic shape was not a consideration.

3. HAPTIC MAGNETIC LEVITATION DEVICE

The new device described here is the first Lorentz magnetic levitation device specifically designed for haptic interaction. Previous research using magnetic levitation fine motion wrists demonstrated the feasibility of Lorentz magnetic levitation for haptic interaction, but also revealed the shortcomings of these positioning devices for haptics. The new design was completed by carefully evaluating desired characteristics for the device and finding a balance among conflicting requirements. Further details of the new magnetic levitation device are available in a design paper.¹⁶

3.1. New Configuration

The small, coupled ranges of translation and rotation in the Magic wrist and UBC wrist (<10 mm and $<10^\circ$) severely limit the user's sensation of interaction and haptic shape perception in the simulated environment. The squat cylindrical shape of both devices makes them awkward to grasp and manipulate, which also reduces the effectiveness of haptic interaction. Ideally, the flotor should be grasped at the center of a rounded shape, so that the range of rotation is equal in all directions and nearly decoupled from translation. The control bandwidths of the IBM and UBC maglev devices could be further increased by reducing the mass and inertia of the flotor, increasing the magnetic forces, and increasing the controller sample rate.

The expected performance parameters of the new device are given in Table 1. The translation range is at least 25 mm in all directions with as much rotation as possible to accommodate the typical fingertip motions for common tool handling tasks. Since the purpose of the device is fine haptic interaction using the fingertips, a larger motion range for arm motion is not necessary. The complete system including the device, amplifiers, power supplies, control processors, network communication, and analog I/O is contained in a single desktop-height cabinet enclosure so that it can be easily rolled up next to a desk and used with a graphical workstation.

The new device flotor is a hemispherical shell with a handle at its center. With this shape, the flotor can be rotated about its center without colliding with the stator. The ranges of rotation and translation are independent and equal in all directions. The flotor coils, the free space around the flotor, and the magnet assemblies in the stator or base all conform to the spherically curved shape. The flotor handle and the top rim of the stator are at the level of the desktop surface. This configuration allows the user's wrist and forearm to rest on the stator rim and desktop while the haptic device handle is manipulated with the fingertips. This position is more comfortable and less tiring for manipulation and results in more sensitive fingertip control for the user since the weight of the hand is supported by the stator. The position of the user's hand during operation of the haptic device is shown in Fig. 3.

The flotor should have minimal levitated mass but high stiffness to avoid flexing. Accordingly, the main body of the flotor is a thin aluminum shell with large oval cutouts for the actuator coils. The coils fit together in a densely packed configuration to maximize the area on the flotor used to generate actuation forces. LEDs for position sensing fit snugly between the coils. The coils are wound from ribbon wire on spherical forms to fit the curvature of the flotor. Although the flotor mass is concentrated in the hemispherical shell, it is still easy to manipulate with one hand since the total mass is low and the weight is supported by actuation forces during use. Figure 4 shows a cutaway representation of the device showing the principal parts including the levitated flotor, the stator enclosure, magnet and sensor assemblies, and the tool handle.

A drawback of Lorentz levitation actuation is that the range of motion of the device is limited by the width of the air gap in the magnetic assemblies. As a result, the range of motion of this device is smaller than most other haptic interface devices. Since the aim of this device is to enable fine, dextrous, local haptic interaction using the fingertips rather than with large-scale arm motions, translation beyond typical fingertip motion for common tool-based tasks was held to be less critical than sensitivity and control bandwidth.

3.2. Actuation

A single Lorentz force actuator consists of two opposing fixed permanent magnet assemblies and an oval wound coil suspended between them in the magnetic circuit air gaps. The Lorentz force \mathbf{f} on the coil is generated in the two air gaps where the coil current loop \mathbf{I} intersects the magnetic flux loop \mathbf{B} and is perpendicular to both the current and the magnetic field vectors. A Lorentz actuator for the new device is shown in Fig. 5 with the associated vectors \mathbf{f} , \mathbf{I} , and \mathbf{B} . The inner and outer magnet assemblies in the new actuators have different widths and the coil is spherically curved in order to conform to the overall hemispherical shape of the new device.

To efficiently generate forces and torques in all directions, the actuator magnets and coils are arranged with three actuators next to the hemisphere rim and the other three positioned halfway down the hemisphere and rotated by 90° . The positions and orientations of the six coil centers on the hemisphere are listed in Table 2 and pictured in Fig. 6, where θ is the angular position from the x axis along the rim, ϕ is the angle down from the hemisphere rim, and ψ is the angle between the long axis of the coil and the hemisphere rim. Each oval-shaped actuator coil spans a $45^\circ \times 61^\circ$ solid angle on the hemisphere. The six oval-shaped curved actuator coils together occupy approximately two-thirds of the flotor area. The flotor shell radius of 115 mm results in large actuator surface areas and forces,

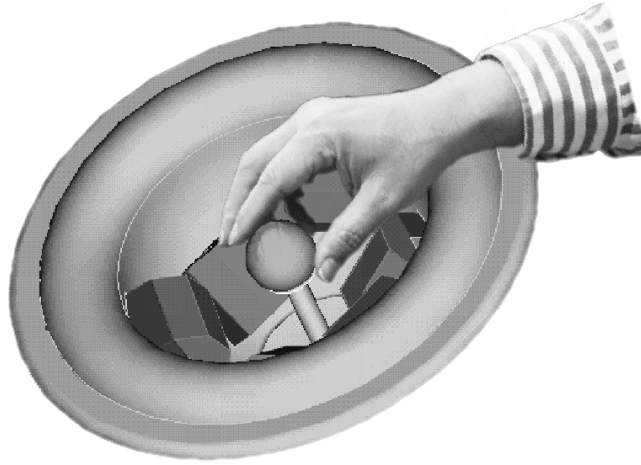


Figure 3. Hand Operation of the Haptic Device

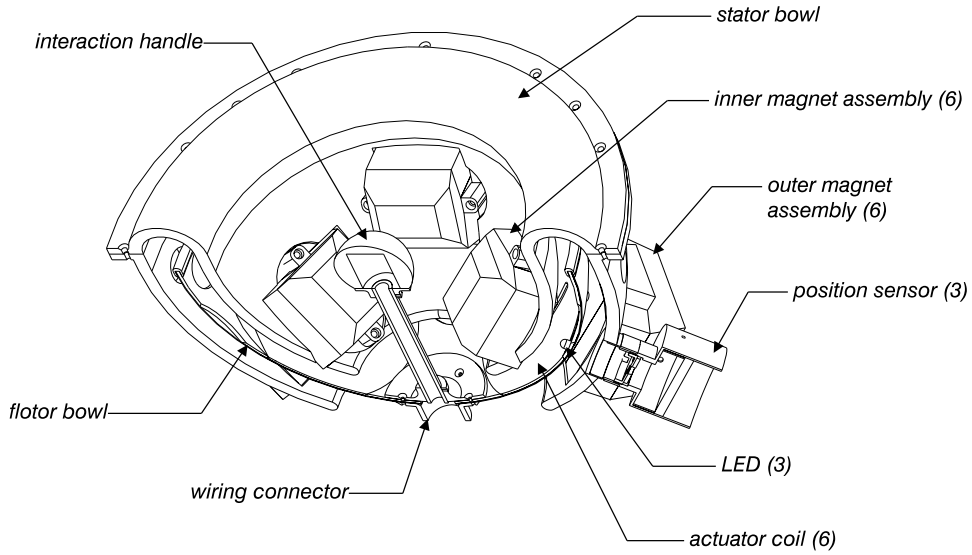


Figure 4. Cutaway View of the Haptic Device

yet allows the levitated mass to be easily manipulated and the entire device to be contained in a deskside cabinet enclosure. The outermost aluminum shell covering the coils adds passive damping to the motion of the flotor due to eddy currents generated by motion through the strong magnetic fields in the stator magnet assembly gaps, which increases the range of stability of the controlled device.

The forces and torques generated on the flotor when it is in the centered position can be expressed as $\mathbf{F} = \mathbf{A}\mathbf{I}$, where $\mathbf{F} = (f_x, f_y, f_z, \tau_x, \tau_y, \tau_z)$ is a 6-vector consisting of the forces and torques exerted on the flotor center in Newtons and N-m, \mathbf{I} a 6-vector of the coil currents in Amperes, and \mathbf{A} the matrix which maps them. \mathbf{A} can be calculated by combining the sums of the Lorentz forces and torques

$$f_i = I_i \times B_i,$$

$$\tau_i = c_i \times f_i,$$

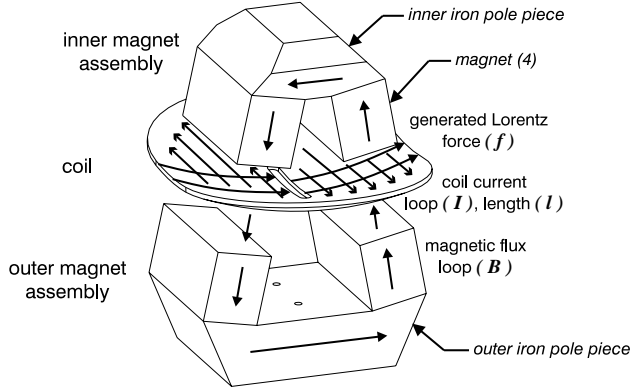


Figure 5. Single Actuator with Magnet Assemblies and Suspended Oval Coil

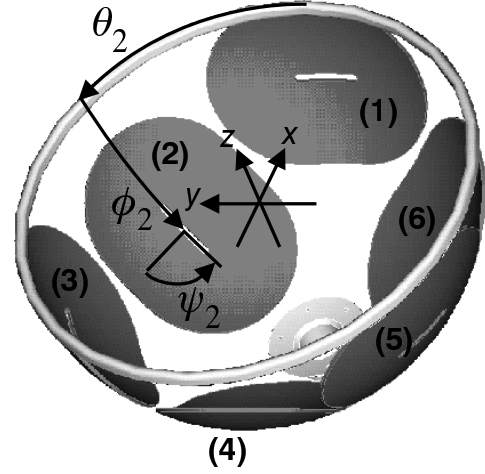


Figure 6. Actuator Coil Configuration on Flotor

Coil	θ	ϕ	ψ
1	0°	22.5°	0°
2	60°	45°	90°
3	120°	22.5°	0°
4	180°	45°	90°
5	240°	22.5°	0°
6	300°	45°	90°

Table 2. Coil Positions on Flotor Hemisphere

where B_i are the magnetic fields of each magnet assembly air gap and c_i are the coil center locations.¹¹ The actuator configuration described above results in the transform matrix:

$$\mathbf{A} = \begin{bmatrix} 2.7553 & -6.2354 & -1.3777 & 0 & -1.3777 & 6.2354 \\ 0 & 3.6000 & 2.3862 & -7.2000 & -2.3862 & 3.6000 \\ 6.6519 & 0 & 6.6519 & 0 & 6.6519 & 0 \\ 0 & 0.2927 & 0.7171 & -0.5855 & -0.7171 & 0.2927 \\ -0.8280 & 0.5070 & 0.4140 & 0 & 0.4140 & -0.5070 \\ 0 & 0.5855 & 0 & 0.5855 & 0 & 0.5855 \end{bmatrix}$$

The steady-state vertical forces necessary to counteract the weight of the levitated flotor are distributed over the three coils next to the hemisphere rim so that the heat generated by the coil resistances is evenly dissipated. Heat dissipation in the actuator coils was a primary concern in the device design since the operating temperature of the coils is the limiting factor for the maximum steady-state forces exertable by the device. Due to this concern, the outer stator bowl was designed with air vents and thermistors were embedded in the flotor coils so that coil temperatures could be monitored during operation.

3.3. Position Sensing

Position is sensed by three large area lateral effect planar position sensitive photodiodes (PSDs) on the fixed outer stator which measure the positions of light spots from three LEDs mounted on the moving flotor. These provide six independent variables (x and y on each sensor) which together determine the position and orientation of the flotor.

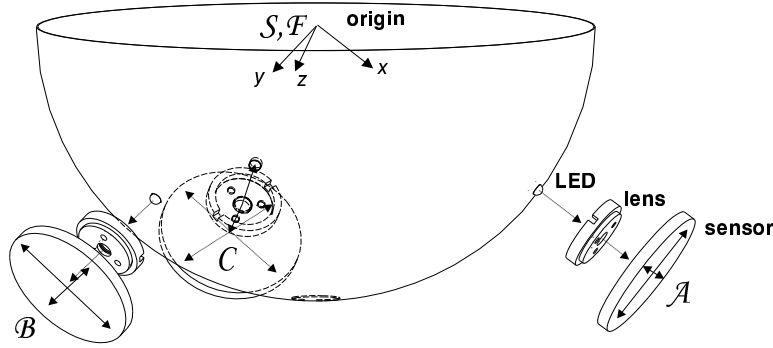


Figure 7. Sensor configuration and Coordinate Frames

The three sensors are equidistant from the stator center and mutually orthogonal to maximize position accuracy and simplify the geometric calculations. The sensor and LED configuration is shown in Fig. 7.

Wide-beam LEDs on the moving flotor are imaged onto the photodiodes by fixed demagnifying lenses since photodiodes sufficiently large and accurate to accommodate the range of motion of the new device with narrow-beam LEDs could not be obtained. A lens demagnification ratio of 1:2.5 at the nominal flotor position maps the full range of motion of the LED onto the limited area of the sensor. The x, y spot position on the sensor determines the angles between the light path and the lens axis. No closed-form solution could be obtained to calculate the Cartesian position and orientation of the flotor from the sensor signals, so iterative solution techniques are used.

4. PERFORMANCE TESTING AND RESULTS

Performance testing of the haptic magnetic levitation device was done to demonstrate the feasibility of the device for realistic haptic interaction. The critical performance parameters for fine, high-performance haptic interaction are the control bandwidths of the device and its sensitivity, or position resolution. The maximum force and stiffness ranges of the device are also given.

After the device assembly was completed, an unforeseen problem with the LEDs on the flotor became apparent: The casings of the LEDs were slightly ferromagnetic, which resulted in large attractive forces on the flotor as the LEDs approach the high magnetic fields of the actuators. These force disturbances made the flotor motion very difficult to control accurately, so the infrared LEDs were replaced with high-brightness red LEDs with no casings and much lower ferrous metal content in the leads, which resulted in greatly improved device performance.

4.1. Maximum Peak Force and Acceleration

The main limitation on the forces obtainable with Lorentz actuation is the heat generated in the coils. With the new hemispherical device, the areas of the coils and flotor hemisphere are large enough to dissipate the heat from the coil currents so that the coils are only very slightly warmer than room temperature during steady-state operation, since only 13.5 W of power is required to cancel gravity on the 850 g flotor. Since the heat dissipation of the coils does not impose such a rigid force limitation for the desktop hemispherical device, the momentary peak forces and accelerations exorable by the device are determined by the current limits of the actuator amplifiers.

The PWM current amplifiers used by the actuators have a 7 A current limit and each actuator generates 7.2 N/A when the coil is centered in the magnetic fields. The maximum peak forces and torques exorable by the device can then be calculated from the current-to-force transform matrix. The resulting maximum forces and torques in each direction individually are: 64 N force in \mathbf{X} , 55 N force in \mathbf{Y} , 140 N force in \mathbf{Z} , 7.3 Nm torque about \mathbf{X} , 6.3 Nm torque about \mathbf{Y} , and 12.2 Nm torque about \mathbf{Z} . These maxima demonstrate that our device has more than adequate force and acceleration capabilities for any reasonable haptic interaction. Since such large forces and accelerations are not needed during typical operation, the maximum actuator currents are limited to 4 A in the control software.

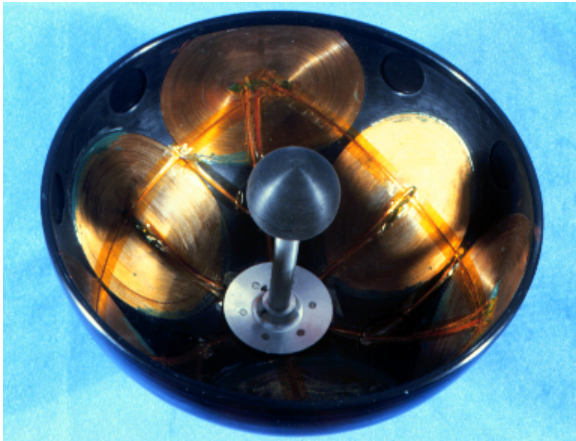


Figure 8. Fabricated Flotor

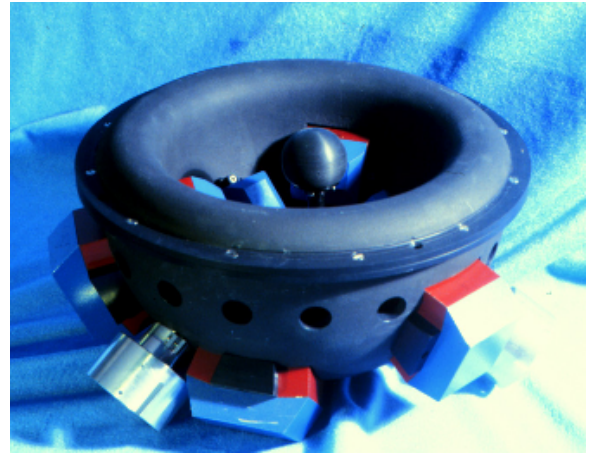


Figure 9. New Fabricated Device

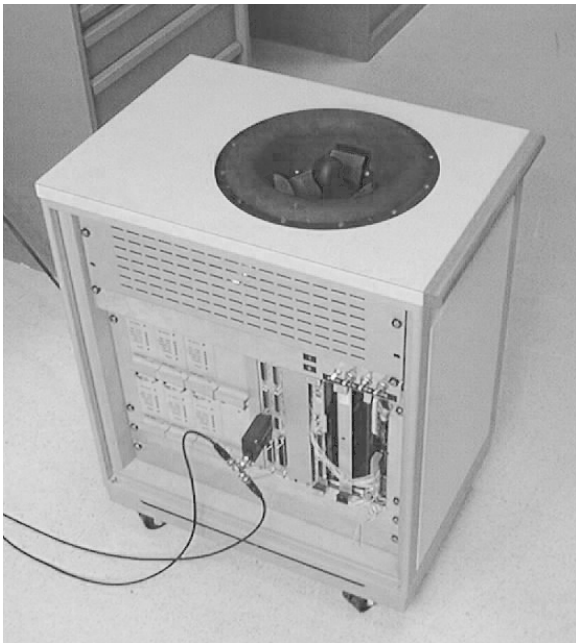


Figure 10. Haptic Interface Device Enclosure

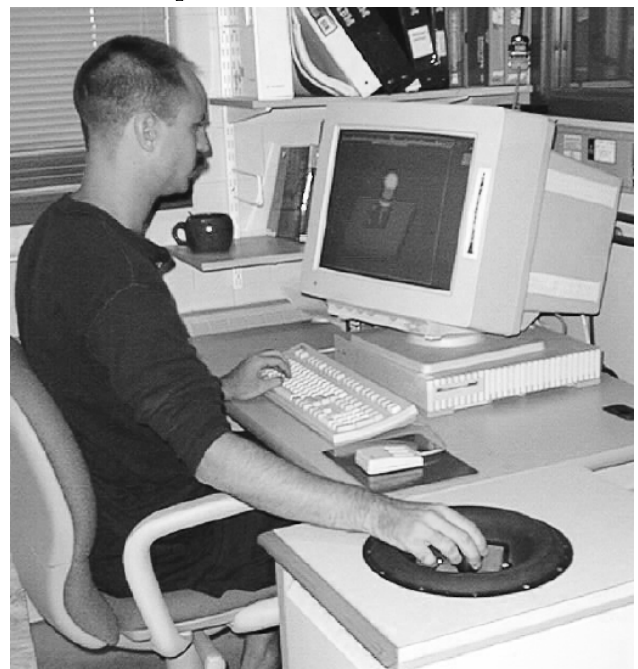


Figure 11. Using the Haptic Interface Device with a Graphics Display

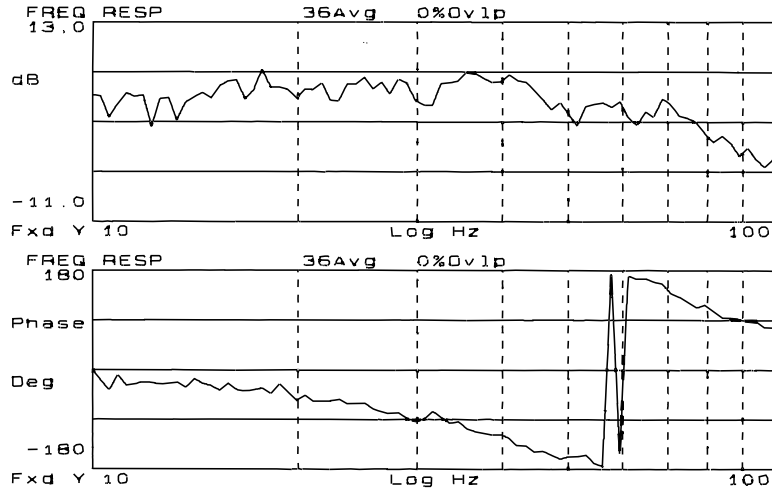


Figure 12. Frequency Response of the Magnetic Levitation Device

4.2. Sensitivity

The position resolution of the sensor system is presently limited to approximately $10\ \mu\text{m}$ due to sensor noise. This resolution level is less precise than the goal of $3\ \mu\text{m}$ given in Table 1, so further efforts will be made to improve the position resolution of the device. Improvements in the sensing and filtering electronics and accurate position estimation using the dynamic and control parameters of the flotor during haptic interaction should improve the effective position resolution somewhat.

4.3. Impedance Range

The maximum stiffnesses that have been achieved with the device to date are $25.0\ \text{N/mm}$ in translation and $50.0\ \text{Nm/rad}$ in rotation, which is sufficiently high to give a user the impression of a rigid surface. Higher stiffnesses are achievable on and around the vertical axis due to greater passive damping with motion in that direction. During free motion the residual stiffness of the device due to the hanging coil current feed wires is approximately $0.005\ \text{N/mm}$, resulting in an maximum to minimum achievable impedance ratio of 5000:1.

4.4. Response Bandwidth

The maximum sample and control rate of the present control system is $1000\ \text{Hz}$. This rate could be increased in the future by using an additional processor board to the VMEbus control system. A dynamic signal analyzer was used to measure the frequency response for small motions of the magnetic levitation device. The magnitude and phase of the response between 10 and $100\ \text{Hz}$ are shown in Fig. 12. As seen in the magnitude response plot, the response remains almost entirely within a $\pm 3\ \text{dB}$ range up to approximately $75\ \text{Hz}$.

5. FUTURE WORK

An aluminum coil flotor is being fabricated to replace the present copper coil flotor, since heat dissipation is less critical than anticipated. Since most of the mass of the flotor is in the coils, an aluminum coil flotor will have approximately half of the mass of the copper coil flotor, the power required to lift the flotor will be greatly reduced, and the motion bandwidth of the entire device can be considerably increased. A new method for controlling spatial impedance which is fully general and exact has been proposed by Fasse¹⁷ and will be implemented for control of the levitated platform.

The operation of this new magnetic levitation haptic interface device is part of an ongoing project to realize high-performance, realistic haptic interaction with dynamic physical simulated environments. Since no other 6 DOF haptic interface device yet exists with the bandwidths of the new device, it will enable evaluation of richer, more subtle methods of haptic interaction with dynamic physical simulations including sophisticated texture and friction

surface effects. A realistic, dynamic virtual environment, integrated with the haptic interface device and a graphical display, will provide users with a very convincing experience of directly interacting with physically real objects in a real environment.

ACKNOWLEDGEMENTS

Zack Butler performed early characterization of the large position sensing photodiodes and designed the sensor circuitry and assemblies. Stella Yu formulated the iterative kinematics solution method used. Our 1996 summer student, Chris Donohue, worked on selection, acquisition and assembly of the enclosure, VMEbus, and power supplies.

REFERENCES

1. K. Shimoga, "A survey of perceptual feedback issues in dexterous telemanipulation: Part i. finger force feedback," in *Proceedings of the IEEE Virtual Reality Annual International Symposium*, pp. 263–270, (New York), January 1993.
2. R. Cholewiak and A. Collins, "Sensory and physiological bases of touch," in *The Psychology of Touch*, M. A. Heller and W. Schiff, eds., Lawrence Erlbaum Associates, Hillsdale, NJ, 1991.
3. R. L. Hollis and S. E. Salcudean, "Lorentz levitation technology: a new approach to fine motion robotics, teleoperation, haptic interfaces, and vibration isolation," in *Proc. 6th Int'l Symposium on Robotics Research*, (Hidden Valley, PA), October 2-5 1993.
4. M. L. Agronin, "The design of a nine-string six-degree-of-freedom force-feedback joystick for telemanipulation," in *Proc. NASA Workshop on Space Telerobotics*, pp. 341–348, 1987.
5. R. Lindemann and D. Tesar, "Construction and demonstration of a 9-string 6 dof force reflecting joystick for telerobotics," in *Proceedings of NASA International Conference on Space Telerobotics*, pp. 55–63, (NASA, Greenbelt, MD), Vol. 4 1989.
6. M. Sato, Y. Hirata, and H. Kawarada, "Space interface device for artificial reality—SPIDAR," *Syst. Comput. Jpn. (USA)* **23**(12), pp. 44–54, 1992.
7. T. Massie and K. Salisbury, "The PHANTom haptic interface: A device for probing virtual objects," in *Proceedings of the ASME Winter Annual Meeting, Symposium on Haptic Interfaces for Virtual Environment and Teleoperator Systems*, (Chicago, Illinois), November 1994.
8. V. Hayward, J. Choksi, G. Lanvin, and C. Ramstein, "Design and multi-objective optimization of a linkage for a haptic interface," in *ARK'94, 4th Int'l Workshop on Advances in Robot Kinematics*, (Ljubljana, Slovenia), June 1994.
9. H. Iwata, "Artificial reality with force-feedback: development of desktop virtual space with compact master manipulator," *Computer Graphics* **24**(4), pp. 165–170, 1990.
10. V. Hayward, "Toward a seven axis haptic device," in *Int'l Conf. on Intelligent Robots and Systems*, pp. 113–139, (Pittsburgh), August 1995.
11. R. L. Hollis, S. Salcudean, and A. P. Allan, "A six degree-of-freedom magnetically levitated variable compliance fine motion wrist: design, modeling, and control," *IEEE Transactions on Robotics and Automation* **7**, pp. 320–332, June 1991.
12. S. Salcudean, N.M. Wong, and R.L. Hollis, "Design and control of a force-reflecting teleoperation system with magnetically levitated master and wrist," *IEEE Transactions on Robotics and Automation* **11**, pp. 844–858, December 1995.
13. P. J. Berkelman, R. L. Hollis, and S. E. Salcudean, "Interacting with virtual environments using a magnetic levitation haptic interface," in *Int'l Conf. on Intelligent Robots and Systems*, (Pittsburgh), August 1995.
14. S. Salcudean and T. Vlaar, "On the emulation of stiff walls and static friction with a magnetically levitated input-output device," in *International Mechanical Engineering Congress and Exposition*, pp. 303–309, (Chicago), November 1994.
15. G. Burdea, *Force and Touch Feedback for Virtual Reality*, Wiley and Sons, Inc., New York, 1996.
16. P. J. Berkelman, Z. J. Butler, and R. L. Hollis, "Design of a hemispherical magnetic levitation haptic interface device," in *Proceedings of the ASME Winter Annual Meeting, Symposium on Haptic Interfaces for Virtual Environment and Teleoperator Systems*, (Atlanta), November 17-22 1996.
17. E. Fasse, "On the spatial compliance of parallel manipulators and levitated platforms," in *ASME IMECE*, (San Diego), April 1997.